The influence of chain constraints on the kinetics of oriented crystallization under low stress

A. J. McHugh* and W. S. Yung
Department of Chemical Engineering, University of Illinois, Urbana, IL 61801, USA
(Received 19 June 1991; revised 26 August 1991; accepted 27 October 1991)

The kinetics of strain-induced crystallization of swollen, crosslinked polyethylene fibres have been measured under low draw conditions ($\alpha = 1.2$ or 1.4) using dynamometry in combination with birefringence. Crosslinking was carried out in dicumyl peroxide to produce a range of chemical and trapped entanglement concentrations. Avrami analysis showed that transformation proceeds by heterogeneous nucleation followed by one-dimensional growth of c-axis oriented crystallites. Growth rates and the size of the corresponding critical nuclei show a strong dependence on crosslink density and entanglement concentration at high crosslink concentration. When entanglement concentration is comparable to the crosslink concentration, the effects of the two constraints become indistinguishable. The latter observation is in line with published results for flow-induced crystallization under comparably low stress levels showing that growth rates are relatively insensitive to entanglement concentration. At higher crosslink concentrations, growth rate decreases in a non-linear fashion indicating potential thermodynamic as well as mobility effects. A physical model illustrates the role of chain constraints on the kinetics of oriented crystallization.

(Keywords: polyethylene; strain-induced crystallization; crosslinking; kinetics)

INTRODUCTION

Although many of the important technological processes for achieving oriented crystallization involve flow, most of our quantitative understanding of the phenomenon is based on analogies with the thermodynamic formalism for strain-induced crystallization (SIC) of crosslinked networks[1]. Studies from our laboratory have been the first to demonstrate quantitative comparisons between the kinetics of SIC of swollen, lightly-crosslinked polyethylene and those of flow-induced crystallization (FIC) from solution[2,3]. Since both transformations take place under relatively low stress levels, the melting point elevation associated with coil deformation is insufficient to sensibly alter the energetics of the rate-controlling nucleation step. On the other hand, chain entanglements play a critical role in the liquid precursor formation that precedes fibre crystallization in FIC[4], and our initial observations suggest that their role in the crystallization is similar to that of chemical crosslinks.

Our most recent study of FIC[5] indicates that the growth kinetics remain constant over a range of temperature, flow rate and molecular weight conditions where differences in entanglement density in the precursor would be expected. This indicates to us that under the low stress levels characteristic of FIC from solution, the nucleation energetics are also insensitive to the degree of chain entanglements. In order to address this further we have measured the SIC kinetics of swollen, polyethylene fibres having a range of chemical crosslinks and physical trapped entanglements under low draw ratio where stress levels are similar to those of FIC ($\sim 10^{-3}$ GPa). Results are presented in this paper along with a physical model to illustrate the role of chain constraints on the oriented transformation.

EXPERIMENTAL

Materials and characterization

Fibre samples were spun from gels of an ultra-high molecular weight polyethylene (Hercules Type 1900, $M_w = 3 \times 10^6$, $M_w/M_n = 1.82$) and crosslinked in dicumyl peroxide following the procedures described in a previous paper[3]. The swelling agent for the crystallization studies was reagent grade xylene. The thermal behaviour of dry and swollen gels was determined using d.s.c. Swollen gels were melted in the presence of xylene at a heating rate of 5°C min^{-1} (to ensure equilibrium between the polymer and the swelling agent) and at 10°C min^{-1} for the dry systems. Wide angle X-ray diffraction patterns of several crystallized fibres were also taken on a Syntex $P2_1$ circle diffractometer equipped with Crystal Logic automation. Patterns showed low degrees of c-axis orientation, indicative of the relatively mild crystallization conditions of these studies.

Characterization of the as-prepared networks included determination of the extent of crosslinking and the amount of physical trapped entanglements from the equilibrium swelling behaviour. Methods of analysis are described by Posthuma de Boer and Pennings[6] and additional details and data are given by Yung[7]. Relevant results are shown in *Figures 1* and *2*. *Figure 1* gives the

*To whom correspondence should be addressed

0032-3861/92/173670-05

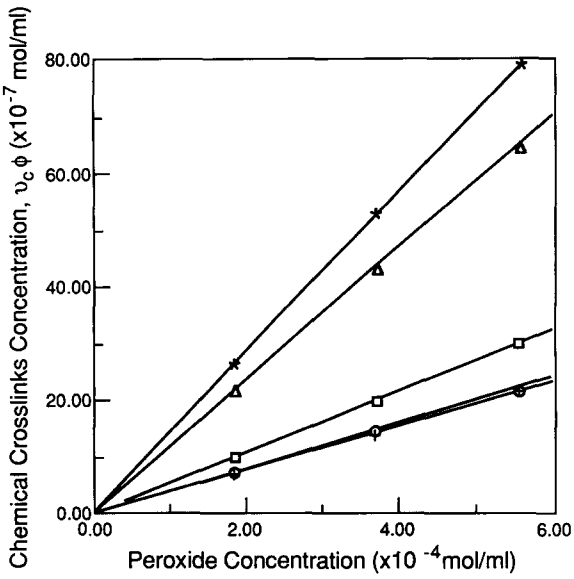

Figure 1 Chemical crosslink concentration in the reaction mixture *versus* peroxide concentration for various polymer concentrations (mol ml^{-1}): ○, 0.05; +, 0.08; □, 0.09; ∗, 0.16; △, 0.18

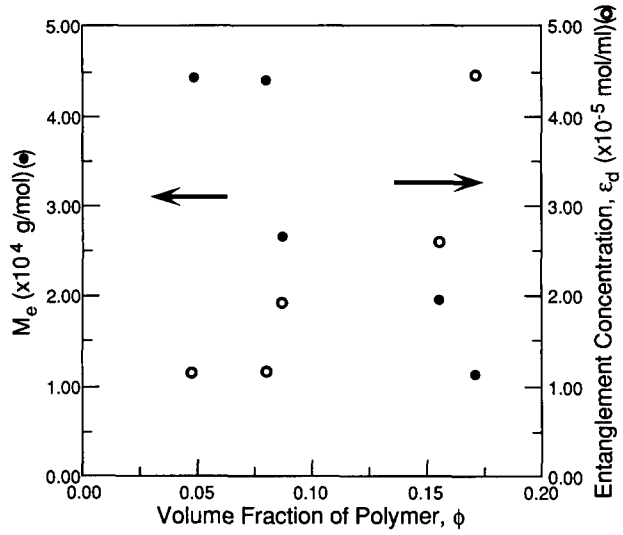

Figure 2 Physical entanglement concentration and average molecular weight between entanglements *versus* polymer volume fraction in the crosslinking reaction mixture

chemical crosslink concentration in the reaction mixture, $v_c\phi$ (where v_c is the chemical crosslink concentration in the dry gel and ϕ is the polymer volume fraction in the reaction mixture), as a function of peroxide concentration in the reaction mixture. *Figure 2* shows the physical entanglement concentration per millilitre of reaction mixture, ε_d, as a function of polymer volume fraction in the crosslinking reaction, and also the average molecular weights between entanglements calculated from the relation[8], $M_e = \rho/2\varepsilon_b$ (where ρ is the polymer density and ε_b is the entanglement density for crosslinking in the bulk state). Using $\varepsilon_b = 2.21 \times 10^{-4}$ mol ml^{-1} from our data gives 2300 for M_e in the undiluted state, which compares favourably to values obtained from melt viscosity[9,10] and loss compliance measurements[8]. Measurements of the retractive force and stress–optical behaviour were also made on undiluted fibres using a dynamometer similar to that described previously[3]. Analysis of the stress–strain behaviour according to the Rivlin–Mooney equation[11], combined with the relationship[12] for the constant C_1, yielded values for the effective chain density, v^*, in good agreement with the swelling results.

Procedures

The dynamometer, optical set-up and video imaging methodology are described in a previous paper[3]. Dried fibres (typically 1 mm in diameter) were immersed in the xylene-filled double-walled vessel until the system reached swelling equilibrium at about 100°C (determined by d.s.c. to correspond to the completely molten state). Senarmont compensation was used as a further check that the network was fully molten. After holding at this temperature for 3 h, fibres were drawn to the desired stretch ratio ($\alpha = 1.2$ or 1.4) at a rate of 5×10^{-5} m s^{-1} to induce amorphous orientation. At this low rate, viscoelastic relaxation was sufficiently rapid to allow simultaneous evaluation of the equilibrium stress–optical behaviour. The resulting plots of birefringence and stress *versus* ($\alpha^2 - 1/\alpha$) exhibited the same linearity found in the previous study[3], hence the stress–optical coefficient was determined from the ratio of the slopes of these curves. Following equilibration, the sample chamber was quenched to the desired crystallization temperature which ranged from 60 to 70°C. Crystallization times ranged from 8 to 24 h, depending on the undercooling.

RESULTS

Fibre birefringence patterns during crystallization were similar to those shown in the previous paper[3]. Under relatively high undercooling conditions multiple fringes formed, while at lower undercoolings the total change in retardation was less than π. Fibre shrinkage due to solvent expulsion also varied with the degree of undercooling. An example of the combined retractive stress, birefringence and fibre diameter data is shown in *Figure 3*. The initial decrease in retractive force on quenching reflects the expected proportionality with temperature. The upturn followed by an increase to the eventual equilibrium is characteristic of the pattern for high undercooling. At lower undercoolings, the retractive stress declined slightly during crystallization without

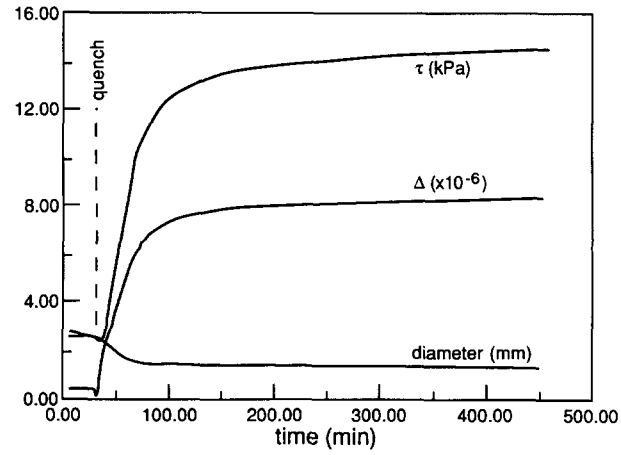

Figure 3 Plots of birefringence (△), stress (τ) and diameter of a swollen fibre during crystallization with the conditions: $T_m/T_c\,\Delta T = 0.0822$ K^{-1}, $v^* = 4.013 \times 10^{-5}$ mol ml^{-1}

exhibiting an upturn. Combined with similar patterns observed in the crystallization of undiluted fibres[7], we conclude that the most likely explanation for the stress upturn effect is the 'tie-molecule' theory proposed by Kawai *et al.*[13].

Crystallization isotherms are analysed according to the Avrami equation:

$$-\ln\left(1-\frac{x}{x_\infty}\right)=\frac{k}{x_\infty}t^n \tag{1}$$

where x is the volume fraction crystallinity and the subscript ∞ refers to the equilibrium state. The relative degree of crystallinity at any time, t, is determined from the total birefringence, Δ, by:

$$\frac{x}{x_\infty}=\frac{\Delta-C\tau}{(\Delta-C\tau)_\infty} \tag{2}$$

where τ is the total stress in the fibre and C is the stress–optical coefficient for the amorphous phase. The validity of this expression has been much discussed in the literature[14–16] and is known to hold at the relatively low strains and crystallinities of our experiments. Measurements of C were extrapolated to the crystallization temperature using the exponential temperature dependence form[17,18] along with a value of 4.561 kJ mol^{-1} for the activation energy[18].

For the range of undercooling conditions studied, Avrami plots displayed well-defined linear regions which were fitted by slopes of unity. This is consistent with our earlier results indicating that the transformation takes place by heterogeneous nucleation with one-dimensional axial growth. *Figure 4* shows data for the relative rate constant at two draw ratios as a function of the undercooling parameter. The relative constant was evaluated from the Avrami intercept, k/x_∞, according to the following expression[3]:

$$k_{rel}=\frac{k \text{ at } T_{c1}}{k \text{ at } T_{c2}}=\frac{\left(\frac{k}{x_\infty}\right)\text{at } T_{c1}}{\left(\frac{k}{x_\infty}\right)\text{at } T_{c2}}\left[\frac{(\Delta-C\tau)_\infty \text{ at } T_{c1}}{(\Delta-C\tau)_\infty \text{ at } T_{c2}}\right] \tag{3}$$

using the value at the crystallization temperature $T_c = 333.8$ K as a reference. As also shown earlier[3], we find that the difference in equilibrium melting point of the stressed, swollen network and that of the unstressed swollen fibre (as determined by d.s.c.) is less than 1°C. Thus the latter T_m values have been used in the undercooling parameter. Since k_{rel} is directly proportional to the growth rate, G, one sees from *Figure 4* that at fixed undercooling, the growth rate decreases with chain density. The corresponding critical growth nucleus length, L, is determined from the slopes of these lines according to the expression[2,3,5]:

$$G \propto \exp\left(-\frac{4L\sigma_s^2}{k_B \Delta H}\frac{T_m}{T_c \Delta T}\right) \tag{4}$$

where ΔH is the crystal heat of fusion, σ_s is the side surface energy of the nucleus and k_B is Boltzmann's constant.

Figure 5 shows L (obtained using standard values for the parameters $\sigma_s = 10 \times 10^{-6}$ J cm^{-2}, $\Delta H = 2.94 \times 10^2$ J cm^{-3}) as a function of the total effective network chain density on a swollen basis, v_s^*. The latter is chosen over the dry basis since it represents the chain density

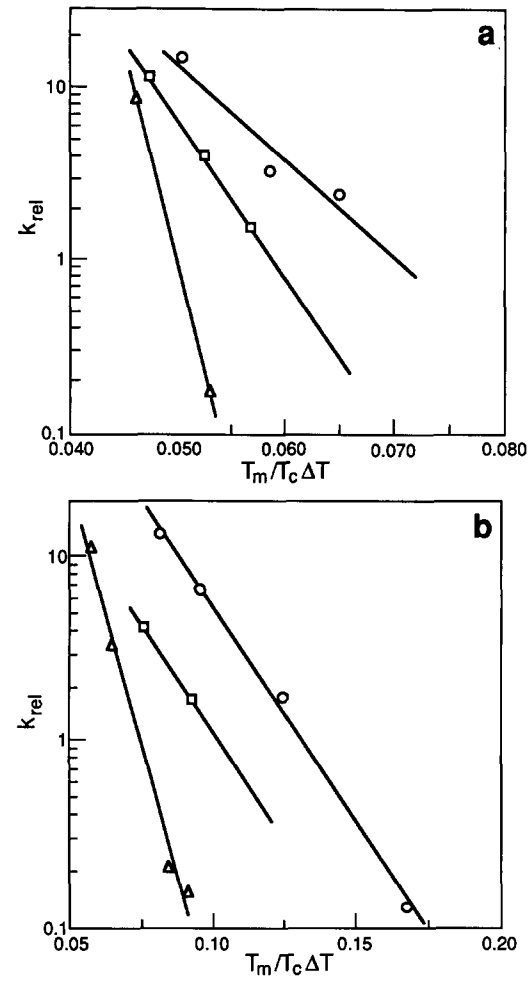

Figure 4 Relative Avrami rate constant as a function of undercooling parameter at two draw ratios. (a) $\alpha = 1.4$; $\varepsilon_s = 0.5 \times 10^{-6}$ mol ml^{-1}; v_s^* ($\times 10^{-6}$ mol ml^{-1}): ○, 2.159; □, 4.499; △, 6.373. (b) $\alpha = 1.2$; $\varepsilon_s = 1.0 \times 10^{-6}$ mol ml^{-1}; v_s^* ($\times 10^{-6}$ mol ml^{-1}): ○, 0.527; □, 2.792; △, 7.296. Values of ε_s and v_s^* are given on a swollen basis

experienced initially by the crystallizing fibre. Lines correspond to values for samples having similar physical entanglement densities, ε_s (on a swollen basis), but different v_s^*. The increase in L with effective network chain density is equivalent to a decrease in the growth rate, G. In the limit where $v_s^* = 2\varepsilon_s$, the formation of the network chains will be due solely to physical entanglements. As indicated in both plots, except for the samples with very high network chain densities, this limit falls in the range 5–8 Å which agrees well with the value of 6 Å found in our FIC study[5]. Thus the length of the growth nucleus remains fairly constant with different entanglement concentrations, i.e. the crystallization kinetics become insensitive to chain density at low chemical crosslink density. Furthermore, since the curves merge smoothly into the range defined by the two dotted lines, the effects of chemical crosslinks and physical entanglements on the growth rate become indistinguishable in the limit of small v_c or when $v_c \approx \varepsilon_d$.

DISCUSSION

With regard to the FIC studies, the findings reported here lead to a consistent interpretation regarding the relative insensitivity of the crystal growth rate to entanglement density. While there is no doubt that chain

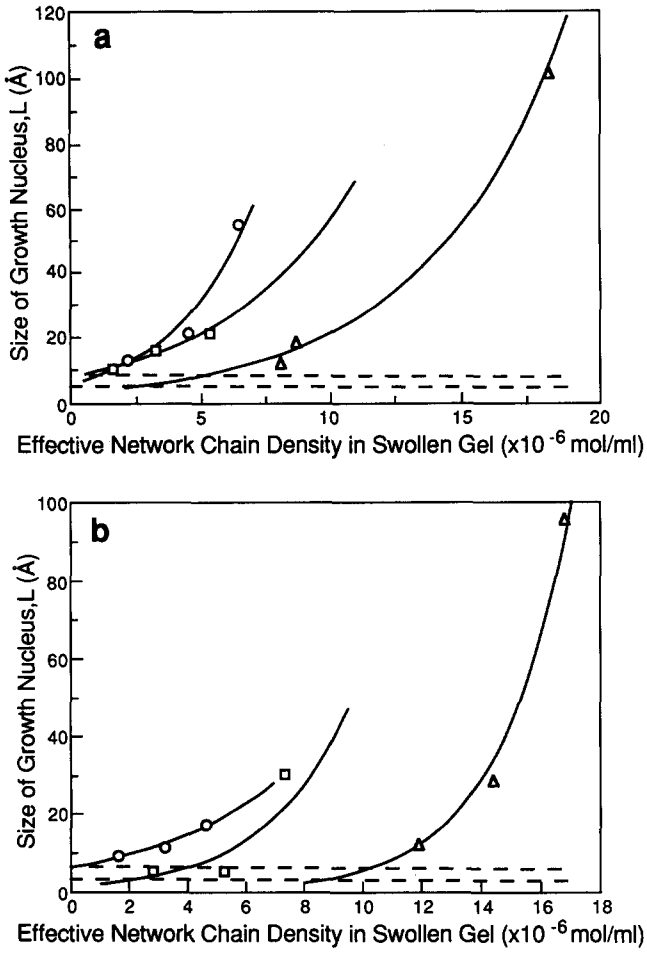

Figure 5 Growth nucleus size as a function of total effective network chain density on a swollen basis. (a) $\alpha = 1.4$; ε_s ($\times 10^{-6}$ mol ml^{-1}): ○, 0.05; □, 1.0; △, 2.5. (b) $\alpha = 1.2$; ε_s ($\times 10^{-6}$ mol ml^{-1}): ○, 0.5; □, 1·0; △, 4.0

entanglements play a critical role in the structure formation leading to precursor phase separation in flowing solutions[4,5,19], it is equally clear that their effect on the crystallization kinetics at low stress is not as pronounced. As an additional observation, *Figure 6* shows endotherm melting peak behaviour of the dry gels as a function of their effective network density. Comparison with *Figure 2* illustrates that the melting temperature is a function of both the crosslink density, ν_c, and the concentration of physical trapped entanglements, ε_b. However the decrease in magnitude of the slopes in *Figure 6* with increasing polymer concentration indicates that the latter have less influence on the melting point depression than do chemical crosslinks. A similar conclusion holds for the heat of fusion. Using the analysis given elsewhere[6] leads to the conclusion that the quantitative influence of chemical crosslinks on the melting point depression is about twice that of physical entanglements[7]. The consistent picture derived relates to the fact that the melting point depression arises from decreases in the availability of crystallizable chain segments (since topological constraints are imperfections which are rejected by the crystal). Since chemical crosslinks are fixed junctions, while physical entanglements have a certain degree of mobility, motion of the latter junction points may allow a wider range of segments for crystal growth.

A qualitative illustration is shown in *Figure 7* which depicts the local interaction of four network chains in the isotropic molten state (*Figure 7a*) and under the influence of an orienting force (*Figure 7b*). Chains A and B are connected to chains a and b by constraints 1 and

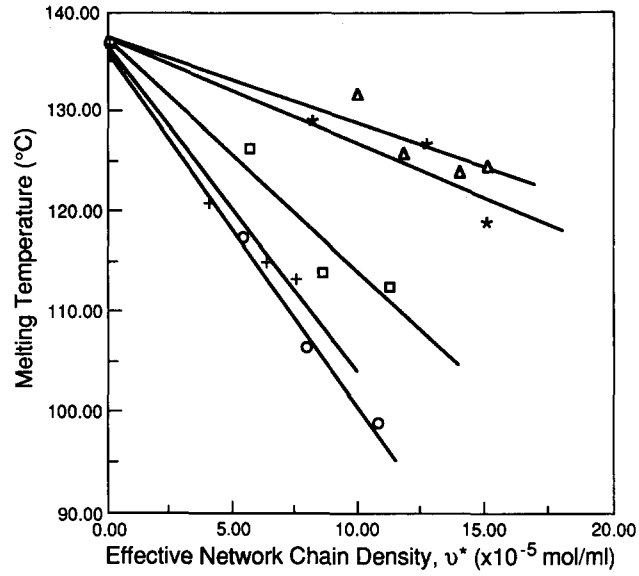

Figure 6 Melting temperature of dry gels *versus* effective network chain density. Polymer concentration (mol ml^{-1}): ○, 0.05; +, 0.08; □, 0.09; ∗, 0.16; △, 0.18

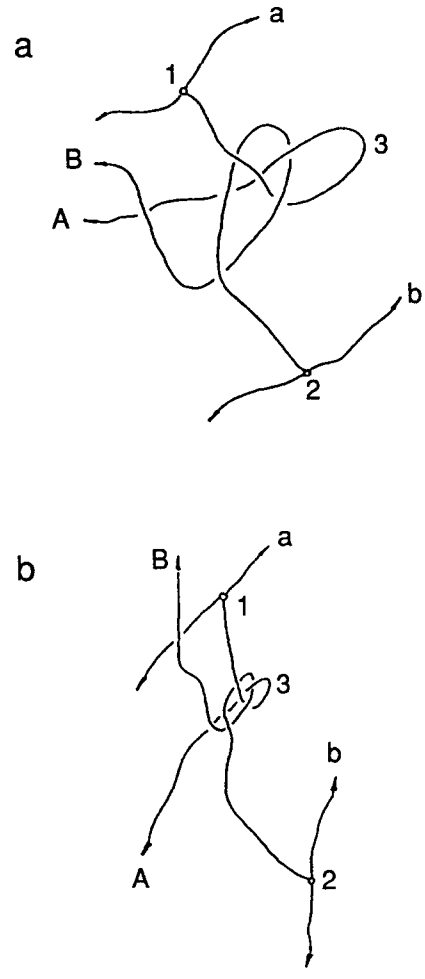

Figure 7 Illustration of local interaction of constraints in four network chains in the isotropic swollen state (a) and under the influence of an orienting force (b)

2 (denoted by small circles) respectively. Considering the arrows as the continuation of the chains, the topological entanglement 3 between A and B cannot be resolved by reptation. In the isotropic state A and B possess thermal energy and a certain degree of motion is possible. Under an orienting force, however, A and B are stretched out and their motions will be restricted by 1 and 2, eventually contributing an extra constraint to the system resembling a transient crosslink (i.e. the ability to restrict local chain motion and to transmit stress to the network). The rate at which this entanglement attains crosslink properties depends on the nature of 1 and 2. If the latter are both entanglements or a combination of entanglement and crosslink (zero or small ν_c) the degree of freedom of 3 will be much higher than in the case when both are chemical crosslinks (high ν_c). In the latter case, since both ends are essentially fixed, no relative motion is possible. Thus, under relatively low orienting forces and chemical crosslink densities, the effects of the two types of constraints become indistinguishable. Likewise the relatively higher chain mobility enhances growth by providing more potential nucleation sites for the growing crystal front. On the other hand, at high chemical crosslink concentration, the constraints become more restrictive (as noted by the melting point depression result) thus inhibiting both the alignment of chains and the corresponding crystal growth. The retardation of crystallization in the presence of crosslinks has also been noted by Gent[20] for pure rubber systems and attributed to a combination of steric and mobility effects.

In addition, thermodynamic constraints may add to the non-linear behaviour at higher crosslink concentrations in *Figure 5*. For example, the theory proposed by Gaylord[21] specifically accounts for the energetics associated with the entropy of strained amorphous segments attached to a growing crystal, as well as the possibility of chain folding at low draw ratios. In the limit of low crystallinity, the initial crystal growth rate predicted by this theory decreases with increasing crosslink density (which is inversely proportional to the number of statistical segments per chain). Different but related arguments based on multiple nucleation and ciliary bridges have also been proposed by Hoffman[22] to describe the energetics of nucleus formation in flow-induced growth. In either case, the net conclusion is that growth rate decreases or corresponding increases in the required nucleus size can be expected for highly constrained oriented systems.

CONCLUSIONS

Based on the results of this work and the related studies discussed, it is apparent that a threshold level of constraints must be present to allow the structure formed by orienting forces to propagate as growth nuclei during oriented crystallization. Under conditions where the constraints are due solely to chain entanglements or where chemical crosslink densities are relatively low, the kinetics of the growth will be relatively insensitive to their concentration. For polyethylene the resulting growth nuclei are on the order of 5–8 Å, while for polypropylene[5] a much larger size is needed (88 Å) which probably reflects the added factor of chain stiffness. Under more constrained conditions, such as high chemical crosslink density, the growth rate will markedly decrease.

The value of the entanglement threshold in flow-induced crystallization should be determined from structural study of the precursor phase separation process and the associated non-linear rheological behaviour of high molecular weight solutions[23]. It seems clear that the ability to regulate entanglement formation in solutions, melts and gels during processing is a critical consideration in the optimization of beneficial properties due to oriented crystallization.

ACKNOWLEDGEMENT

A portion of this work was completed while one of us (W.S.Y.) was supported under a Fellowship from The Plastics Institute of America.

REFERENCES

1 McHugh, A. J. *Polym. Eng. Sci.* 1982, **22**, 15
2 McHugh, A. J. and Spevacek, J. A. *J. Polym. Sci., Polym. Lett. Edn* 1987, **25**, 105
3 McHugh, A. J. and Yung, W. S. *J. Polym. Sci., Polym. Phys. Edn* 1989, **27**, 431
4 McHugh, A. J. and Blunk, R. H. *Macromolecules* 1986, **19**, 1249
5 McHugh, A. J. and Spevacek, J. A. *J. Polym. Sci., Polym. Phys. Edn* 1991 **29**, 969
6 Posthuma de Boer, A. and Pennings, A. J. *J. Polym. Sci., Polym. Phys. Edn* 1976, **14**, 187; *Faraday Disc. Chem. Soc.* 1979, **68**, 345
7 Yung, W. S. PhD Thesis, University of Illinois, 1991
8 Ferry, J. D. 'Viscoelastic Properties of Polymers', 3rd Edn, Wiley, New York, 1980, Ch. 13
9 Schreiber, H. P., Bagley, E. B. and West, D. C. *Polymer* 1963, **4**, 355
10 Porter, R. S. and MacKnight, W. J. *Rubber Chem. Technol.* 1968, **4**, 1
11 Posthuma de Boer, A. and Pennings, A. J. *Macromolecules* 1977, **10**, 981
12 Mark, J. E. *Adv. Polym. Sci.* 1982, **44**, 1
13 Kawai, T., Iguchi, M. and Tonami, H. *Kolloid Z.* 1967, **221**, 28
14 Stein, R. S. and Norris, F. H. *J. Polym. Sci.* 1956, **21**, 381
15 Hashiyama, M., Gaylord, R. and Stein, R. S. *Makromol. Chem. Suppl.* 1975, **1**, 579
16 Smith, K. J. *J. Polym. Sci. A-2* 1968, **6**, 1723
17 Saunders, D. W., Lightfoot, D. R. and Parsons, D. A. *J. Polym. Sci., A-2* 1968, **6**, 1183
18 Morgan, R. J. and Treloar, L. R. G. *J. Polym. Sci., A-2* 1972, **10**, 51
19 Vrahopoulou, E. P. and McHugh, A. J. *J. Rheol.* 1987, **31**, 361; *J. Non-Newtonian Fluid Mech.* 1987, **25**, 157; *Chem. Eng. Commun.* 1987, **57**, 289
20 Gent, A. N. *J. Polym. Sci.* 1955, **18**, 321
21 Gaylord, R. J. *J. Polym. Sci., Polym. Phys. Edn* 1976, **14**, 1827
22 Hoffman, J. D. *J. Res. Nat. Bur. Stand. (US)* 1979, **83A**, 359
23 Kishbaugh, A. J. PhD Thesis, University of Illinois, 1992